Electron spin transport in graphene and carbon nanotubes

Tombros, Nikolaos

5

The magneto-Coulomb effect in spin valve devices[1]

Abstract

We discuss the influence of the magneto-Coulomb effect (MCE) on the magnetoconductance of spin valve devices. We show that MCE can induce magnetoconductances of several per cents or more, dependent on the strength of the Coulomb blockade. Furthermore, the MCE-induced magnetoconductance changes sign as a function of gate voltage. We emphasize the importance of separating conductance changes induced by MCE from those due to spin accumulation in spin valve devices.

[1]Published as: S. J. van der Molen, N. Tombros and B. J. van Wees, *Phys. Rev. B* **73**, 220406 (2006)

5.1 Introduction

The recent past has seen an impressive effort in connecting ferromagnetic leads to ever smaller non-ferromagnetic structures. The main idea behind this is to make use of the electron spin for device purposes. In a two-terminal, spin valve geometry, a resistance difference ΔR is expected between two basic situations. First, if the two ferromagnetic leads are magnetized in an anti-parallel fashion, the majority spin species injected at the first ferromagnet is predominantly reflected at the second ferromagnet. This results in a high resistance state. On the other hand, in the case of parallel magnetizations, the injected majority spin couples well to the second ferromagnet, leading to a lower resistance state. With the miniaturization of the central structure, quantum confinement effects come into play. Recently, quite some progress has been made in studying spin devices in the presence of Coulomb blockade [1–11]. The interpretation of the two-terminal data in these reports has mostly focused on spin transport and spin accumulation. Here, we discuss another influence on the two-terminal resistance in ferromagnetically contacted nanostructures, namely the magneto-Coulomb effect (MCE) discovered by Ono *et al.* [12].

5.2 Magneto-Coulomb effect, definition

In this contribution, we consider a confined conductor weakly connected to two ferromagnets, F_1 and F_2 (see Fig. 5.1a). The coupling is described by two sets of resistances and capacitances, R_1, C_1 and R_2, C_2, respectively. Furthermore, the island can be gated by a voltage V_g via a capacitor C_g. For a basic introduction to the MCE, we first concentrate on one of the ferromagnets only, F_1, which is assumed magnetized in the positive direction. Let us suppose that a positive external magnetic field, $B > 0$, is applied. In that case, the energy of the spin up ($\uparrow$) and spin down ($\downarrow$) electrons shifts by the Zeeman energy, in opposite directions (see Fig. 5.1b). However, for a ferromagnet, the density of states of both spin species differs ($N^{\uparrow} > N^{\downarrow}$). Hence, a shift in the chemical potential $\Delta\mu$ needs to take place to keep the number of electrons constant [12]:

$$\Delta\mu = -\frac{1}{2} P g \mu_B B \tag{5.1}$$

where the thermodynamic polarization P is defined as $P = \frac{N^{\uparrow} - N^{\downarrow}}{N^{\uparrow} + N^{\downarrow}}$, g is the gyromagnetic ratio and μ_B is the Bohr magneton. For MCE one should consider the thermodynamic quantity P. This P differs considerably from the polarization determined in tunnel experiments. For the latter, tunnel matrix elements play a

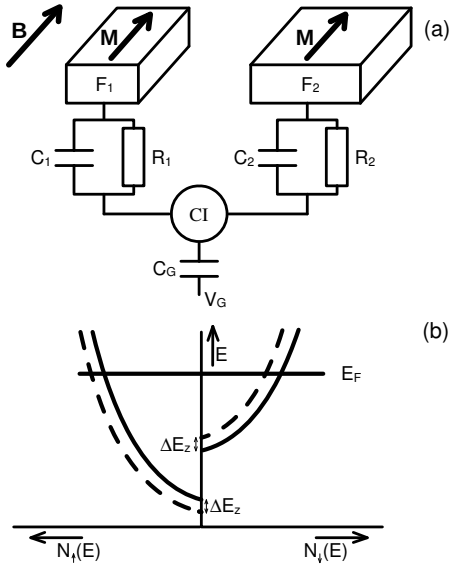

Figure 5.1: a) Sample structure considered. Two ferromagnetic strips, F_1 and F_2, with coercive fields B_{c1} and B_{c2} are weakly connected to a Coulomb island (CI) via two tunnel barriers (resistances R_1 and R_2 and capacitances C_1 and C_2). Furthermore, a gate connects capacitively to the island (C_G). b) Sketch of the density of states N of the two spin species in a ferromagnet, versus energy. When a magnetic field is applied, the energies of the two spin species shift (ΔE_z) in opposite directions by the Zeeman effect. Since $N^{\uparrow} > N^{\downarrow}$, this results in a change in the work function, ΔW.

role as well. For Co, $P \approx -0.6$, whereas for Ni, $P \approx -0.8$, see Ref. [12]. In practice, the ferromagnet will be attached to a macroscopic non-magnetic lead. This demands equal chemical potentials in both metals. Hence, the energy shift in the ferromagnet translates to a change in the contact potential between the ferromagnet and the normal metal, $\Delta\phi$, according to, $-e\Delta\phi = -\Delta\mu$ [12]. Equivalently, one could say that the work function of the ferromagnet changes by $\Delta W = -\Delta\mu$. Since the ferromagnet is weakly coupled to the central island, this shift influences the Coulomb levels of the latter. In fact, an additional charge Δq is induced onto the island due to the contact potential change $\Delta\phi$. Applying a magnetic field thus has an effect that is similar to changing the gate voltage. This equivalence has been beautifully demonstrated by Ono *et al.* [12] For the situation sketched above, we find:

$$\Delta q(B) = \frac{C_1}{2e} P g \mu_B B \tag{5.2}$$

Hence, if no magnetization rotation or switching takes place in the ferromagnet, the induced charge onto the island changes linearly with the applied field B. In the Coulomb blockade regime, the conductance G is a function of (induced) charge. Hence, we find that the conductance changes when a field is applied:

$$G(q, B) = G(q) + \frac{dG}{dq}\Delta q(B) \tag{5.3}$$

Here q denotes the charge state of the island at zero field. For a Coulomb island, $G(q)$ and $\frac{dG}{dq}$ can be calculated or measured. The exact theory to apply depends on the magnitude of the various energy scales involved [13]. The sign of the magneto-conductance is determined by the signs of both P and $\frac{dG}{dq}$. We note that the function $G(q)$ is periodic. Hence, $\frac{dG}{dq}$ changes sign periodically.

5.3 Magneto-Coulomb effect, magnetization switching

Next, we incorporate magnetization switching. Again, we start with ferromagnet F_1 magnetized in the positive direction, but now we ramp down the external field ($B < 0$). Then, according to eq. A.3, the conductance changes linearly with B, as long as the magnetization of the ferromagnet is unchanged. However, when B reaches the coercive field, i.e., $B = -B_c$, the magnetization of the ferromagnet switches to the negative direction. Hence, also Δq changes discontinuously, by $\Delta q_c = \frac{C_1}{e} P g \mu_B B_c$. This results in a jump in the conductance via eq. A.3. For more negative B fields, the conductance change will be linear with B again, but now with opposite sign. So far, we have considered an island connected to one ferromagnet only. The extension to a spin valve device with two ferromagnetic contacts is rather trivial, since their effects can be added. Summarizing, a conductance change linear in B is expected, with discontinuities at the coercive fields of both ferromagnets.

To illustrate the above, we consider the device in Fig. 5.1a, where F_1 and F_2 have different switching fields. Experimentally, this can be achieved by choosing thin strips of different widths [14–16]. To calculate the conductance properties at zero field, we use the orthodox model of Coulomb blockade [13]. We assume each Coulomb peak to be independent. Although this is not exact, it suffices to show the principle of MCE. We note also that eq. A.3 can in principle be used for other Coulomb regimes. In Fig. 5.2a, we show $G(q)$ for a certain choice of parameters (see caption Fig. 5.2). We use q as a relative quantity, i.e., $q = 0$ corresponds to an initial situation with N electrons on the island (charge $-Ne$).

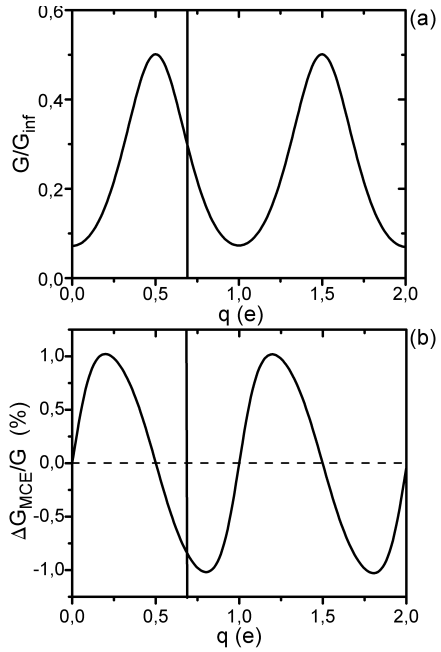

Figure 5.2: a) Conductance G vs charge state q for the system in Fig. 5.1a. G is calculated with the orthodox model. Parameters: $C_1 = C_2 = 2 \cdot 10^{-17} F, C_g = 5 \cdot 10^{-18} F, R_1 = R_2 = 2.5 M\Omega$. G is given in units of $G_\infty = 1/(R_1 + R_2) = 0.2 \mu S$. b) Relative conductance change $\Delta G_{MCE}/G$ vs q (in %). $\Delta G_{MCE}(q)$ equals the total change in conductance due to magnetization switching of the ferromagnetic electrodes. This quantity is defined in Fig. 5.3b for a specific choice of q ($q = 0.69e$, also indicated in a) and b)). We use $P = -0.6$, $g = 2$ and $T = 4.2K$.

A change in q by e corresponds to a change in Coulomb level energy by e^2/C_{tot} (where C_{tot} is the total capacitance of the island). Next, we will determine the field dependence of the conductance, using eq. A.3. For this, we need $\frac{dG}{dq}$, which we derive from Fig. 5.2a. Furthermore, one requires $\Delta q(B)$, the charge induced as a result of the B-field. This function is shown in Fig. 5.3a. It is calculated using $P = -0.6$, which is the thermodynamic polarization of cobalt [12]. As discussed above, discontinuities in $\Delta q(B)$ are found at the respective coercive fields of the two ferromagnetic electrodes. To obtain G vs B, we combine eq. A.3 with Figs. 5.2a and 5.3a. In Fig. 5.3b, we show a typical result, evaluated around $q = 0.69e$. We find indeed that MCE gives linear conductance changes for fields exceeding the switching fields. Around the switching fields, discontinuities occur, leading to hysteretic behavior. We note that Fig. 5.3b does show similarities with several experiments in spin valve devices. This emphasizes the importance to separate

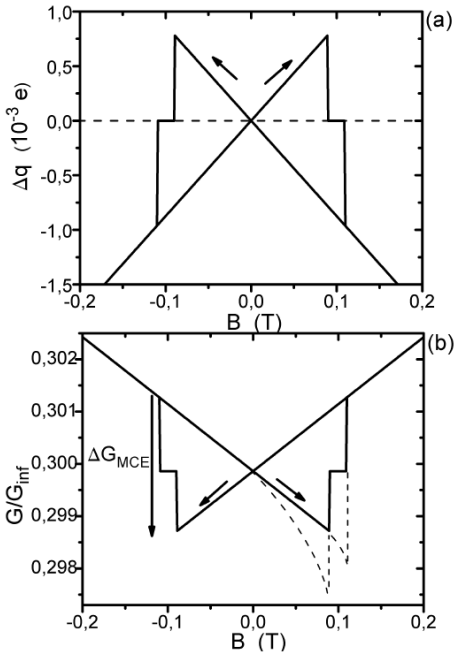

Figure 5.3: a) Induced charge on the island, Δq, vs B-field (see eq.A.2). Δq varies linearly with B, except at the switching fields, where steps are seen. The curve ignores the demagnetizing field. b) Conductance vs B-field calculated using eq. A.3, Fig. a) and Fig. 5.2a (at $q = 0.69e$, indicated in Fig. 5.2). Solid line: demagnetization field ignored. The sum of the steps is defined as $\Delta G_{MCE} < 0$. With this, we construct Fig. 5.2b. Dashed line: qualitative effect of the rotation of the demagnetization field at the nanotube (only drawn for positive fields). We use $B_{c1} = 0.09T$ and $B_{c2} = 0.11T$

both phenomena [16].

Finally, we evaluate the size of MCE for various q. For this, we concentrate on the discontinuities in Fig. 5.3b. We define the conductance change due to MCE, $\Delta G_{MCE}(q)$, as the sum of the two conductance steps at the coercive fields, i.e., $\Delta G_{MCE}(q) = -\frac{dG}{dq} P g \mu_B (C_1 B_{c1} + C_2 B_{c2})/e$. We indicate $\Delta G_{MCE}(q = 0.69e)$ in Fig. 5.3b. In Fig. 5.2b, we plot the relative magnetoconductance change $\Delta G_{MCE}/G$ as a function of q. Inspecting the graph, we infer that both sign and magnitude of MCE depend critically on q. The reason is that $\Delta G_{MCE}/G$ is roughly proportional to the derivative of the logarithm of $G(q)$. We note that Fig. 5.2b changes considerably for a sample with a non-zero background conductance. Hence, $\Delta G_{MCE}/G$ changes sign where $G(q)$ reaches its extremes. Furthermore, $\Delta G_{MCE}/G$ reaches its minima and maxima close to the inflection points

of $G(q)$. The latter has an important consequence. The sharper the Coulomb peaks get, the higher the maximum conductance change due to MCE becomes. Consequently, even small Δq can induce sizeable effects, *without* a fundamental limitation. In Fig. 5.2a, we obtain a maximum conductance change of 1%. We note that the system in Figs. 5.2 and 5.3 is comparable to the single wall carbon nanotubes, measured by Kim et al. [7]. They have $G = 0.37\mu S$ at 4.5 K, and find $\Delta G/G \approx 1.5\%$. However, in principle, effects exceeding 100% are also possible. Indeed, MCE depends strongly on the system parameters, which define the sharpness of the Coulomb peaks.

5.4 Magneto-Coulomb effect in a carbon nanotube

Recently, much work has been done to investigate magnetic field induced conductance changes in quantum dot-like structures, such as carbon nanotubes [1–4, 7–11, 17] and small metal islands [5, 6]. In these studies, conductance changes are seen that are interpreted in terms of spin accumulation. However, three phenomena are noteworthy: 1) in many cases, the change in conductance sets in before the magnetic field changes sign, i.e. before the ferromagnetic electrodes switch their magnetization [1–5,18]. 2) In some studies the magnetoconductance changes sign as a function of gate voltage [2, 4, 17, 18]. 3) In carbon nanotubes connected to only one ferromagnet (and to gold), field-induced conductance changes are also observed [19]. In the latter system spin detection is clearly not possible.
We believe that in many experiments, MCE plays an important role. As seen in Figs. 5.2 and 5.3, MCE-induced conductance changes have the following properties: 1) they set in continuously at zero field; 2) they change sign as a function of gate voltage, exactly at the Coulomb peaks; 3) MCE-induced conductance changes also take place for Coulomb islands connected to only one ferromagnet, as discussed above. Hence, the combination of MCE with spin accumulation could be responsible for part of the phenomena listed above. We note that the sign changes seen in Refs. [2, 4, 17, 18] have been explained within coherent spin transport models (see also Ref. [20]). However, in most of these systems Coulomb blockade was also observed. This implies that MCE should be taken into account to obtain full correspondence between experiment and theory.

It is important to separate spin accumulation from magnetoresistance effects such as MCE. The best way to do this is by a direct measurement, using a non-local, four-probe geometry [16]. If a non-local measurement is not possible, the MCE and spin accumulation should be separated in other ways. For example by monitoring the temperature and gate voltage dependence of the relative conductance changes and comparing these data sets to what is expected for MCE.

Clearly, MCE decreases with a decrease of the conductance peaks. Otherwise, experiments on nanotubes with two ferromagnetic contacts can be compared to those with one ferromagnet and a normal metal [4]. However, for a proper comparison, it is essential, that the coupling to the normal metal and the ferromagnet is very similar.

5.5 Discussion and conclussions

Finally, we discuss the influence of a demagnetizing field on the MCE qualitatively. This field may play a significant role in carbon nanotubes onto which a ferromagnetic strip is evaporated. Locally, in the nanotube beneath the ferromagnet, the demagnetizing field is expected to be quite high, of order 0.5 T (assuming a field due to the ferromagnet of 1 T close to its surface). The reason for this is that the aspect ratio of the nanotube is unity in the radial direction. The demagnetizing field shifts the local work function of the ferromagnet thus adding to MCE. Suppose now that the ferromagnet is magnetized in the positive direction and a negative B field is applied. Then, we expect the ferromagnetic domains in the vicinity of the nanotube to change their orientation slowly. This locally rotates the demagnetization field and therefore changes Δq. As a consequence, a characteristic magnetoconductance trace is expected, with conductance changes setting in *before* the ferromagnet actually switches (cf. Ref. [21]). As soon as the ferromagnet does switch, we are in a mirror image of the original situation and the contribution of the demagnetizing field jumps back to its old value. We conclude that MCE due to the demagnetizing field gives a continuous conductance change for fields down to the coercive field. Just as for the external-field-induced MCE, conductance changes are already expected at fields close to 0 T. This is consistent with the majority of two-terminal experiments [1–6, 18]. In Fig. 5.3b, we sketch the total MCE, including that of the demagnitizing field (dashed line). We note the similarity of the full MCE curve with what is expected for spin accumulation. For asymmetric contacts (e.g., $C_1 \neq C_2$), the shape of Fig. 5.3b will change accordingly. If one of the jumps dominates, only one peak may be observed experimentally.

In summary, we show that the magneto-Coulomb effect should be taken into account to explain experiments on spin valve structures in the Coulomb blockade regime. A proper separation of spin accumulation and MCE is essential for a good understanding of the first.

References

[1] K. Tsukagoshi, B. W. Alphenaar and H. Ago, *Nature* **401** 572 (1999).

[2] K. Tsukagoshi and B. W. Alphenaar, *Superlattices and Microstructures* **27**, 565 (2000).

[3] S. Sahoo, *et al.*, *Appl. Phys. Lett.* **86**, 112109 (2005)

[4] S. Sahoo, *et al.*, *Nature Phys.* **1**, 99 (2005)

[5] K. Yakushiji, *et al.*, *Nature* **4**, 57 (2005)

[6] L. J. Zhang, *et al.*, *Phys. Rev. B* **72**, 155445 (2005)

[7] J. R. Kim, *et al.*, *Phys. Rev. B.* **66**, 233401 (2002).

[8] S. Chakraborty, *et al.*, *App. Phys. Lett* **83**, 1008 (2003).

[9] D. Orgassa, G. J. Mankey and H. Fujiwara, *Nanotechnology* **12**, 281 (2001).

[10] B. Zhao, *et al.*, *J. Appl. Phys.* **91**, 7026 (2002)

[11] B. W. Alphenaar, S. Chakraborty and K. Tsukagoshi, in *Electron Transport in Quantum Dots* (Kluwer Academic/Plenum Publishers, New York 2003) chap. 11.

[12] K. Ono, H. Shimada and Y. Ootuka, *J. Phys. Soc. Jpn* **67**, 2852 (1998); H. Shimada, K. Ono, and Y. Ootuka, *J. Appl. Phys.* **93**(10), 8259 (2003), H. Shimada and Y. Ootuka, *Phys. Rev. B* **64**, 235418 (2001)

[13] L. P. Kouwenhoven, *et al.*, Electron transport in quantum dots, Proc. Adv. Study Institute on Mesoscopic Electron transport (L.L. Sohn, L.P. Kouwenhoven and G. Scön, Eds), Kluwer 1997

[14] M. Johnson and R. H. Silsbee, *Phys. Rev. Lett.* **55**, 1790 (1985)

[15] F. J. Jedema, A. T. Filip and B. J. van Wees, *Nature* **410**, 345 (2001).

[16] N. Tombros, S. J. van der Molen and B. J. van Wees, *Phys. Rev. B*, **73**, 233403 (2006)

[17] H. T. Man, L. J. W. Wever and A. F. Morpurgo, *preprint*, cond-mat/0512505 v1

[18] B. Nagabhirava, *et al.*, *preprint*, cond-mat/0510112

[19] A. Jensen, *et al.*, *Phys. Rev. B* **72**, 035419 (2005)

[20] A. Cottet, *et al.*, EuroPhys. Lett. **74**, 320 (2006)

[21] M. Brands and G. Dumpich *J. Appl. Phys.* **97**, 114311 (2005)